



Inclined Magnetic Field and Viscous Dissipation Effects on Tangent Hyperbolic Nanofluid Flow with Zero Normal Flux of Nanoparticles at the Stretching Surface

N Saidulu¹, T Gangaiah² and A Venkata Lakshmi³

¹Department of Mathematics, Osmania University, Hyderabad, Tealnagana, India

²Department of Mathematics, Govt. Degree College, Mancherial, Telangana, India

³Department of Mathematics, UCT, Osmania University, Hyderabad, Telangan, India
nampellysaidulu28@gmail.com

ABSTRACT

This article presents the effect of inclined magnetic field on the MHD boundary layer flow of tangent hyperbolic fluid with nanoparticles past a stretching surface with viscous dissipation, chemical reaction and convective boundary condition. Condition of zero normal flux of nanoparticles on the wall is used for the concentration boundary condition, which is the current topic that have yet to be studied extensively. The partial differential systems are reduced to ordinary differential systems by using appropriate similarity transformations. The reduced systems are solved numerically by Runge-Kutta fourth order method with shooting technique. The velocity, temperature and nanoparticle volume fraction profiles are discussed for different physical parameters. As well as the Skin friction, Nusselt and Sherwood numbers are exhibited and analyzed. It is found that the viscous dissipation enhances the effective thermal diffusivity and the temperature rises. It is also observed that the inclined magnetic force decreases the velocity field, showing an increasing behavior of temperature and nanoparticle volume fraction profiles.

Key words: MHD, Tangent hyperbolic Nanofluid, Zero normal flux, Inclined magnetic field, Viscous dissipation.

INTRODUCTION

The momentum and heat transfer of the boundary layer flow over a stretching surface have been applied in numerous chemical engineering processes, such as polymer extrusion processes and metallurgical processes, which involve cooling of a molten liquid. Sakiadis [1] initiated studying the boundary layer flow over a stretched surface moving with a constant velocity and formulated boundary layer equations for two dimensional and axisymmetric flows. Crane [2] investigated the flow caused by a stretching sheet. On the other hand, Gupta [3] stressed that realistically, stretching surface is not necessarily continuous. Magyari and Keller [4] analyzed the steady boundary layers on an exponentially stretching continuous surface with an exponential temperature distribution. Elbashbeshy [5] investigated the heat transfer over an exponentially stretching continuous surface with suction. Fathizadeh *et al* [6] proposed a powerful modification of the homotopy perturbation method for MHD flow over a stretching sheet. The most important non-Newtonian liquid model is tangent hyperbolic liquid model and which has certain advantages over other non-Newtonian formulations. Pop and Ingham [7] presented the tangent hyperbolic fluid model and it is extensively used in different laboratory experiments. After that, Nadeem *et al* [8] studied the peristaltic transport of a hyperbolic tangent fluid within an asymmetric channel. The tangent hyperbolic fluid model is used by Friedman *et al* [9] for large-scale magneto-rheological fluid damper coils. In another study, peristaltic flow of tangent hyperbolic fluid in a curved channel is studied by Nadeem *et al* [10] and they explored the behavior of various parameters on pressure rise against flow rate and plotted stream lines to understand the pattern of the flow. Akbar *et al* [11] investigated the steady MHD flow of tangent hyperbolic fluid over a stretching sheet. They found that velocity profile decreases by increasing power law index and Weissenberg number but demonstrates opposite results for skin friction.

A nanofluid is a liquid containing nanometer-sized solid particles, called nanoparticles, which basically increasing thermal conductivity of the base fluids according to an investigation of Choi [12]. Pak and Cho [13] ascribed the increased heat transfer coefficients noticed in nanofluids to the dispersion of suspended particles. Xuan and Li [14]

proposed that the heat transfer enhancement was the result of the increase in turbulence induced by nanoparticle motion. A large amount of literature is available, which deals with studying nanofluids and their applications [15–17]. Akram and Nadeem [18] investigated the impact of peristaltic transport of a tangent hyperbolic fluid in the presence of nanoparticles under the influence of inclined magnetic field. They have found that increase in the Brownian motion and thermophoresis leads to enhance temperature profile. Saidulu and Lakshmi [19] described the boundary layer flow of a non-Newtonian Casson fluid accompanied by heat and mass transfer towards an exponentially stretching sheet with viscous dissipation and chemical reaction. Bala [20] investigated the theoretical study of the steady two-dimensional MHD convective boundary layer flow of a Casson fluid over an exponentially inclined permeable stretching surface in the presence of thermal radiation and chemical reaction. Prabhakar *et al* [21] analyzed the effect of inclined Lorentz forces on hyperbolic tangent nanofluid flow with zero normal flux of nanoparticles at the stretching sheet. Recently, many researchers discussed the tangent hyperbolic fluid flows over stretching surfaces [22–28].

The aim of the present study is to investigate the numerical solution of the tangent hyperbolic nanofluid over a sheet with viscous dissipation, chemical reaction and convective boundary condition. Using similarity transformations, the partial differential equations are reduced to a set of nonlinear ordinary differential equations, which are solved by Runge-Kutta fourth order method with shooting technique. Graphical results are plotted and discussed for various parameters on the velocity, temperature, and concentration profiles.

MATHEMATICAL FORMULATION

Consider the steady two-dimensional boundary layer flow of an incompressible viscous and electrically conducting tangent hyperbolic nanofluid flow over a stretching surface which coincides with the plane $y = 0$. The fluid flow is confined to $y > 0$. The x -axis is taken along the stretching sheet in the direction of motion while the y -axis is perpendicular to the sheet. Two equal and opposite forces are applied along the x -axis so that the wall is stretched keeping the origin fixed. The flow takes place in the upper half plane $y > 0$. Along with this we considered an inclined magnetic field, viscous dissipation and chemical reaction to the flow.

The constitutive equation of tangent hyperbolic fluid is:

$$\bar{\tau} = \left[\mu_{\infty} + (\mu_0 + \mu_{\infty}) \tanh(\Gamma \bar{\gamma})^n \right] \bar{\gamma}, \quad (1)$$

in the above expression $\bar{\tau}$ is an extra stress tensor, μ_{∞} is an infinite shear rate viscosity, μ_0 is the zero shear rate viscosity, Γ is the time-dependent material constant, n is the power law index i.e. flow-behavior index and $\bar{\gamma}$ defined as:

$$\bar{\gamma} = \sqrt{\frac{1}{2} \sum_i \sum_j \bar{\gamma}_{ij} \bar{\gamma}_{ji}} = \sqrt{\frac{1}{2} \Pi} \quad (2)$$

where $\Pi = \frac{1}{2} \text{tr} \left(\text{grad}V + (\text{grad}V)^T \right)^2$. We consider Eq. 1, for the case when $\mu_{\infty} = 0$ because it is not possible to discuss the problem for the infinite shear rate viscosity and since we are considering tangent hyperbolic fluid that describing shear thinning effects so $\Gamma \bar{\gamma} < 1$. Then Eq. 1 takes the following form:

$$\bar{\tau} = \mu_0 \left[(\Gamma \bar{\gamma})^n \right] \bar{\gamma} = \mu_0 \left[(1 + \Gamma \bar{\gamma} - 1)^n \right] \bar{\gamma} = \mu_0 \left[1 + n(\Gamma \bar{\gamma} - 1) \right] \bar{\gamma}. \quad (3)$$

The governing equations for the tangent hyperbolic fluid model after applying the boundary layer approximations can be defined as follows

$$\frac{\partial u}{\partial x} + \frac{\partial v}{\partial y} = 0, \quad (4)$$

$$u \frac{\partial u}{\partial x} + v \frac{\partial u}{\partial y} = \nu (1-n) \frac{\partial^2 u}{\partial y^2} + \sqrt{2} \nu n \Gamma \left(\frac{\partial u}{\partial y} \right) \frac{\partial^2 u}{\partial y^2} - \frac{\sigma B^2 u}{\rho} \sin^2(\gamma), \quad (5)$$

$$u \frac{\partial T}{\partial x} + v \frac{\partial T}{\partial y} = \frac{k}{\rho c_p} \frac{\partial^2 T}{\partial y^2} + (1-n) \frac{\mu}{\rho c_p} \left(\frac{\partial u}{\partial y} \right)^2 + \frac{\Gamma n}{\sqrt{2}} \frac{\mu}{\rho c_p} \left(\frac{\partial u}{\partial y} \right)^3 + \tau \left\{ D_B \frac{\partial C}{\partial y} \frac{\partial T}{\partial y} + \frac{D_T}{T_{\infty}} \left(\frac{\partial T}{\partial y} \right)^2 \right\}, \quad (6)$$

$$u \frac{\partial C}{\partial x} + v \frac{\partial C}{\partial y} = D_B \frac{\partial^2 C}{\partial y^2} + \left(\frac{D_T}{T_{\infty}} \right) \frac{\partial^2 T}{\partial y^2} - k_1 (C - C_{\infty}). \quad (7)$$

The corresponding boundary conditions are:

$$u = U, \quad v = -V, \quad -k \frac{\partial T}{\partial y} = h_f (T_f - T), \quad D_B \frac{\partial C}{\partial y} + \frac{D_T}{T_\infty} \frac{\partial T}{\partial y} = 0 \quad \text{at } y = 0 \quad (\text{zero normal flux}), \quad (8)$$

$$u \rightarrow 0, \quad T = T_\infty, \quad C = C_\infty \quad \text{as } y \rightarrow \infty. \quad (9)$$

Where u and v are the velocities in the x - and y directions, respectively, $\nu = \frac{\mu}{\rho}$ is the kinematic viscosity, ρ is the fluid density (assumed constant), μ is the coefficient of fluid viscosity, σ is the electrical conductivity, $B(x)$ is variable magnetic field, γ is an inclination angle, k is the thermal conductivity, T is the fluid temperature, T_∞ is constant temperature of the fluid in the viscid free stream, c_p is the specific heat at constant pressure, $\tau = \frac{(\rho c)_p}{(\rho c)_f}$ is the ratio between the effective heat capacity of the nanoparticle material to the heat capacity of the base fluid, ρ_p is the density of the particles, c_f is the volumetric expansion coefficient, C is the nanoparticle volume fraction, D_B is the Brownian diffusion coefficient, and D_T is the thermophoretic diffusion coefficient and k_1 is reaction rate. $U = ax$ is the stretching velocity, T_f is the convective fluid temperature below the moving sheet, h_f the convective heat transfer coefficient, $V > 0$ is the velocity of suction and $V < 0$ is the velocity of blowing.

Method of Solution

Introducing the similarity variables as

$$\eta = \sqrt{\frac{a}{\nu}} y, \quad u = axf'(\eta), \quad v = -\sqrt{av}f(\eta), \quad (10)$$

$$\theta(\eta) = \frac{T - T_\infty}{T_f - T_\infty}, \quad \phi(\eta) = \frac{C - C_\infty}{C_\infty}.$$

Where η is the similarity variable, $f(\eta)$ is the dimensionless stream function, $\theta(\eta)$ is the dimensionless temperature, $\phi(\eta)$ is the dimensionless concentration and primes denote differentiation with respect to η . The transformed ordinary differential equations are:

$$(1-n)f'''' + ff'' - (f')^2 + nWef''f'''' - M\sin^2(\gamma)f' = 0, \quad (11)$$

$$\frac{1}{Pr}\theta'' + f\theta' + (1-n)Ec(f'')^2 + \frac{n}{2}WeEc(f'')^3 + Nb\theta'\phi' + Nt(\theta')^2 = 0, \quad (12)$$

$$\phi'' + LePrf\phi' + \frac{Nt}{Nb}\theta'' - LePrK_1\phi = 0, \quad (13)$$

and the boundary conditions take the following form:

$$f(0) = S, \quad f'(0) = 1, \quad \theta'(0) = Bi(\theta(0) - 1), \quad Nb\phi'(0) + Nt\theta'(0) = 0, \quad (14)$$

$$f'(\eta) \rightarrow 0, \quad \theta(\eta) \rightarrow 0, \quad \phi(\eta) \rightarrow 0 \quad \text{as } \eta \rightarrow \infty. \quad (15)$$

where the prime denotes differentiation with respect to η , $M = \frac{\sigma B^2}{\rho a}$ is the magnetic parameter, $We = \sqrt{\frac{2a}{\nu}}\Gamma U$ is

the Weissenberg number, $S = -\frac{V}{\sqrt{av}} > 0$ or (< 0) is the suction (or blowing) parameter, $Pr = \frac{\mu c_p}{k}$ is the Prandtl

number, $Le = \frac{\alpha}{D_B}$ is Lewis number, $\alpha = \frac{k}{\rho c_p}$ is the thermal diffusivity, $Bi = \frac{h_f}{k} \sqrt{\frac{\nu}{a}}$ is the Biot number,

$Nb = \frac{\tau D_B C_\infty}{\nu}$ is the Brownian motion parameter, $Nt = \frac{\tau D_T (T_f - T_\infty)}{T_\infty \nu}$ is the thermophoresis parameter,

$Ec = \frac{U^2}{c_p (T_f - T_\infty)}$ is an Eckert number and $K_1 = \frac{k_1}{a}$ is the chemical reaction parameter. The important physical

quantities of this problem are the skin friction coefficient C_{f_x} and the local Nusselt number Nu_x , which represent the wall shear stress and the heat transfer rate respectively.

The skin friction coefficient C_{f_x} is given by

$$C_{f_x} Re_x^{\frac{1}{2}} = \left((1-n)f''(\eta) + \frac{n}{2} We (f''(\eta))^2 \right)_{\eta=0}, \tag{16}$$

and the local Nusselt number Nu_x is given by

$$Nu_x Re_x^{-\frac{1}{2}} = -\theta'(0), \tag{17}$$

Here $Re_x = \frac{Ux}{\nu}$ is a local Reynold number.

NUMERICAL PROCEDURE

The system of coupled non-linear ordinary differential equations (11) - (13) along with the boundary conditions (14) and (15), which are solved numerically by Runge-Kutta fourth order method with shooting technique. The step size taken as $\Delta\eta = 0.01$ is used to obtain the numerical solution, and the boundary condition $\eta \rightarrow \infty$ is approximated by $\eta_{max} = 10$. The solutions are obtained with an absolute error tolerance of 10^{-6} in all cases. In order to get a clear insight of physical problem, numerical results are displayed with the help of graphical illustrations. Also, to calculate the accuracy of the present numerical results, comparison with those obtained by Fathizadeh et al [6] are shown in Table 1.

Table-1 Values of skin friction coefficient for several values of magnetic parameter M in the absence of $n = Ec = K_I = Bi = S = \gamma = Nb = Nt = Le = 0$

M	Numerically	HPM [6]	Present study
0	-1	-1	-1.000008
1	-1.41421	-1.41421	-1.414214
5	-2.44948	-2.44948	-2.449490
10	-3.31662	-3.31662	-3.316625
50	-7.14142	-7.14142	-7.141428

RESULTS AND DISCUSSION

This section is focused on the physical insight of different parameters on the velocity $f'(\eta)$, temperature $\theta(\eta)$ and nanoparticle volume fraction profiles $\phi(\eta)$. Figures 1a and 1b show the effect of the power law index n on the velocity, temperature and nanoparticle volume fraction profiles. Here, the velocity and the associated boundary layer thickness show reducing but the reverse behavior is obtained for temperature and nanoparticle volume fraction profiles with larger values of the power law index n . The effect of the magnetic parameter M on the velocity, temperature and nanoparticle volume fraction profiles are shown in Figs. 2a and 2b. It is seen that the velocity is a decreasing function of the magnetic field parameter M . It holds because with the increase in M , the Lorentz force increases which produces the retarding effect on the fluid velocity. From Fig. 2b the effect of magnetic field is to enhance the temperature and nanoparticle volume fraction profiles. Clearly, larger magnetic parameter yields larger Lorentz force which causes strong resistance in the fluid motion. Hence, more heat is produced which enhances the temperature and nanoparticle volume fraction profiles.

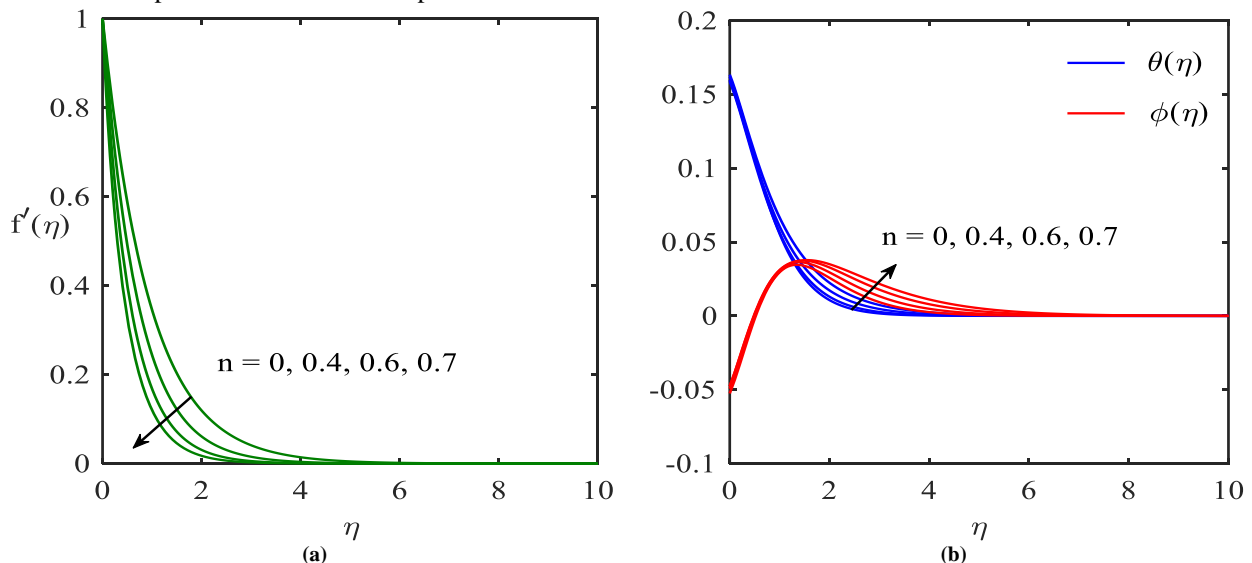


Fig. 1 Effect of n on (a) velocity and (b) temperature and nanoparticle volume fraction profiles

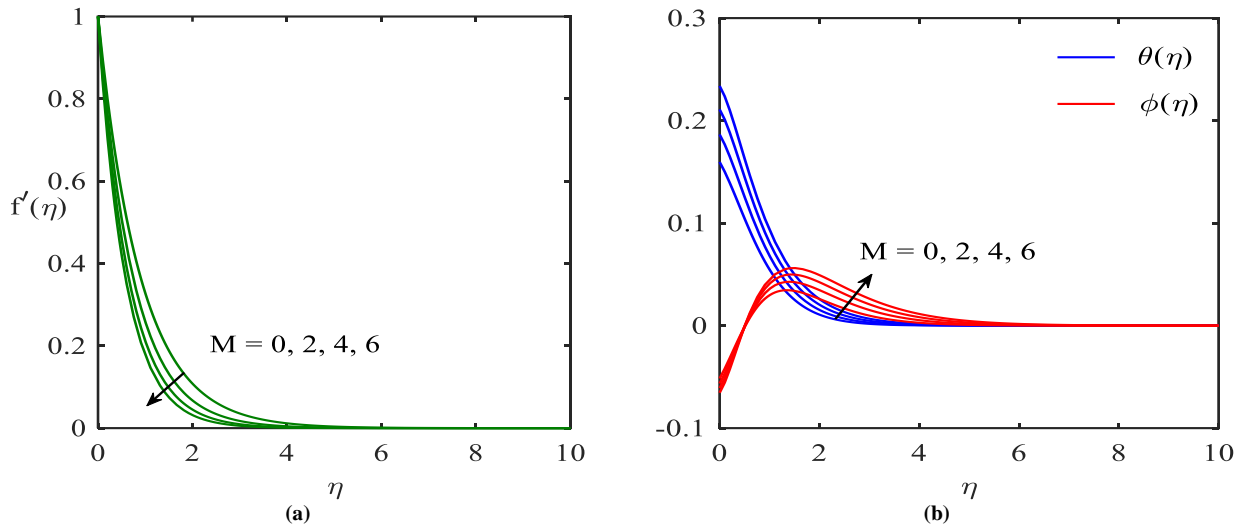


Fig. 2 Effect of M on (a) velocity and (b) temperature and nanoparticle volume fraction profiles

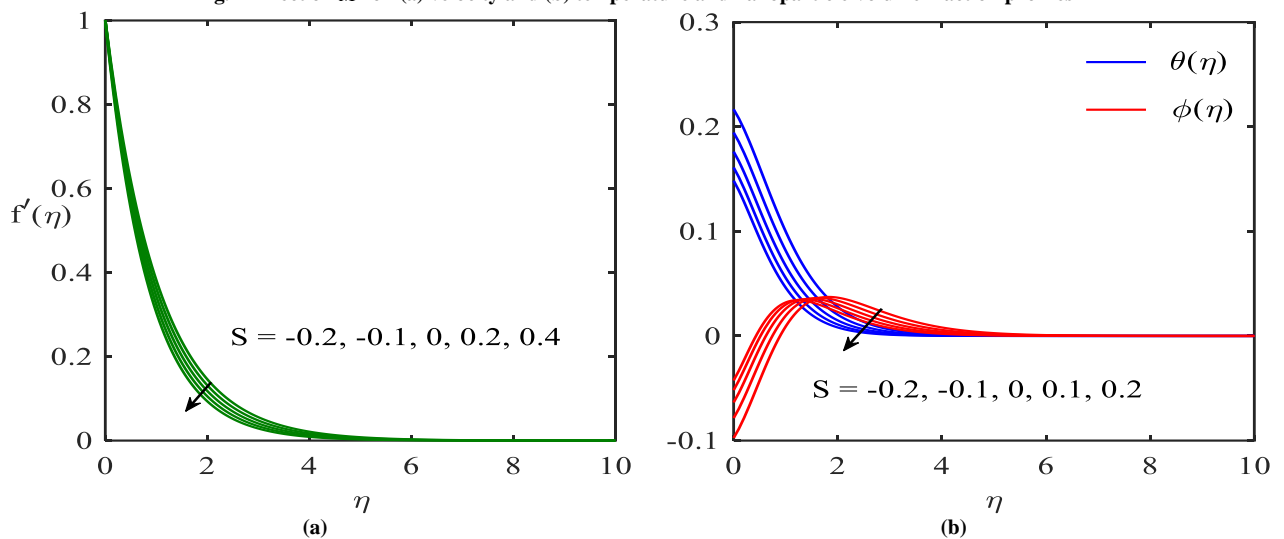


Fig. 3 Effect of S on (a) velocity and (b) temperature and nanoparticle volume fraction profiles

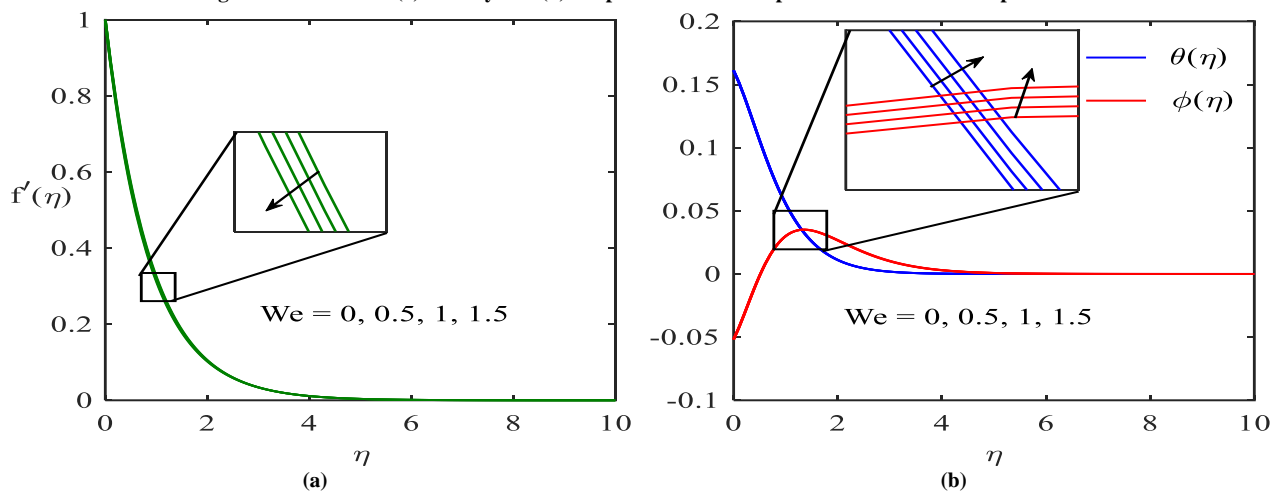


Fig. 4 Effect of We on (a) velocity and (b) temperature and nanoparticle volume fraction profiles

The effects of the suction/blowing parameter S on the velocity, temperature and nanoparticle volume fraction profiles have been analyzed and the results are presented in Figs. 3a and 3b. These figures show that the suction/blowing has a profound effect on the boundary layer thickness in which the suction reduces the thermal boundary layer thickness whereas blowing thickens it. However, the net effect for the suction parameter is to slow down the flow velocity, temperature and nanoparticle volume fraction but the reverse is true for the blowing parameter. So, we can conclude that the suction can be effectively used for the fast cooling of the sheet.

Figures 4a and 4b indicate the effect of the Weissenberg number We on the velocity, temperature and nanoparticle volume fraction profiles. It is observed that the velocity profile decreases by the increasing We . In fact, it is a ratio between the shear rate time and the relaxation time. Hence, for larger Weissenberg numbers We , the fluid becomes thicker, and consequently, the velocity and the boundary layer thickness decrease. Hence velocity profile shows the decreasing behavior while temperature and nanoparticle volume fraction profiles are increasing with increasing values of Weissenberg number We . Figures 5a and 5b give the insight for the influence of the angle of inclination on the velocity, temperature and nanoparticle volume fraction profiles. It is noted that with the increase in γ , the velocity profile increases but the reverse behavior is obtained for temperature and nanoparticle volume fraction profiles. This phenomenon often occurs due to strengthens in the applied magnetic field. Due to enhanced magnetic field an opposite force is produced to the flow, called Lorentz force which resists the fluid flow; consequently, the velocity profile decreases. It is also seen that for the angle $\gamma = 0$ the magnetic field has not effect on the velocity profile, while maximum resistance is offered for the fluid particles when $\gamma = \pi/2$.

Figure 6a shows the impact of convective parameter called Biot number Bi on the temperature and nanoparticle volume fraction profiles. Physically Biot number is the ratio of convection at the surface to conduction within the surface of a body. It holds that both temperature and nanoparticle volume fraction profiles are increasing with an increasing values of Biot number Bi . Figure 6b indicates the effect of the viscous dissipation parameter Ec on the temperature and nanoparticle volume fraction profiles. It is seen that the temperature and nanoparticle volume fraction profiles are increasing functions of the viscous dissipation parameter Ec .

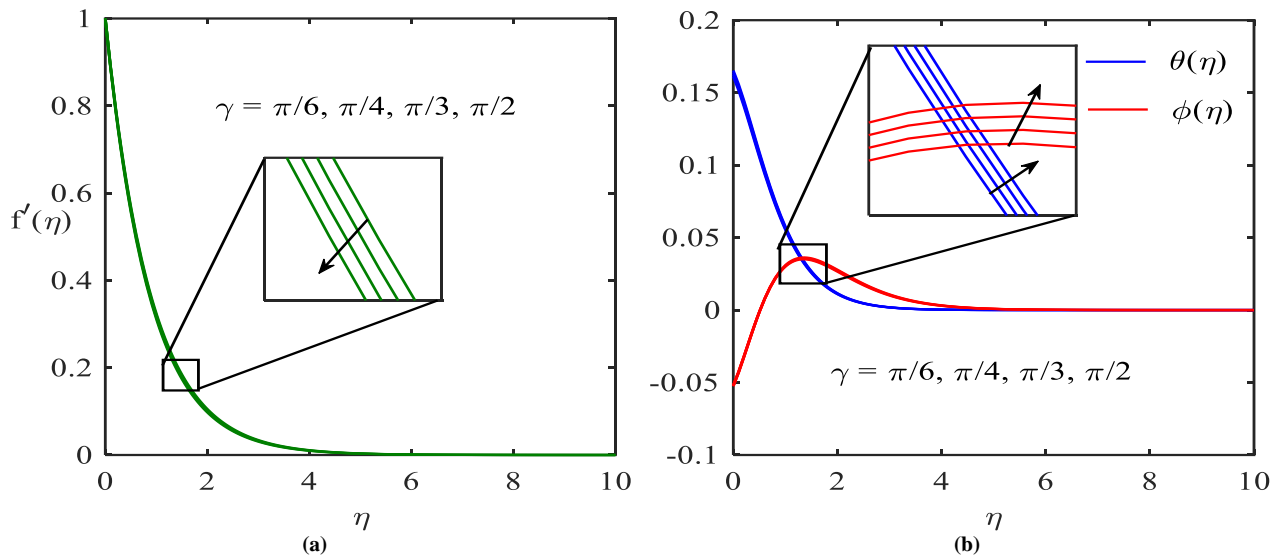


Fig. 5 Effect of γ on (a) velocity and (b) temperature and nanoparticle volume fraction profiles

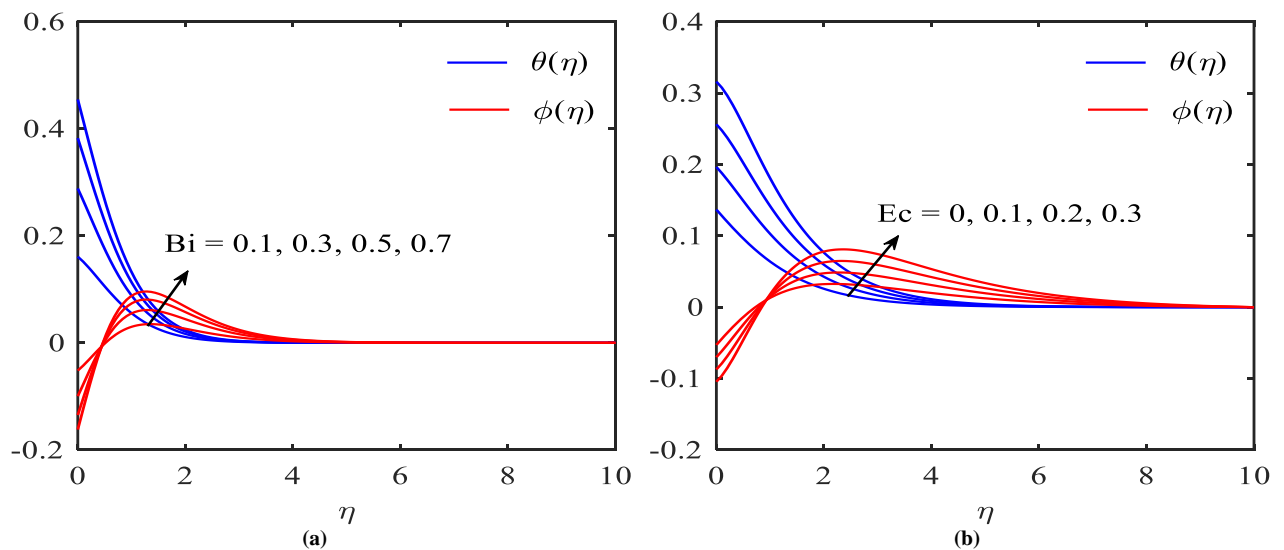


Fig. 6 Effects of Bi and Ec on temperature and nanoparticle volume fraction profiles

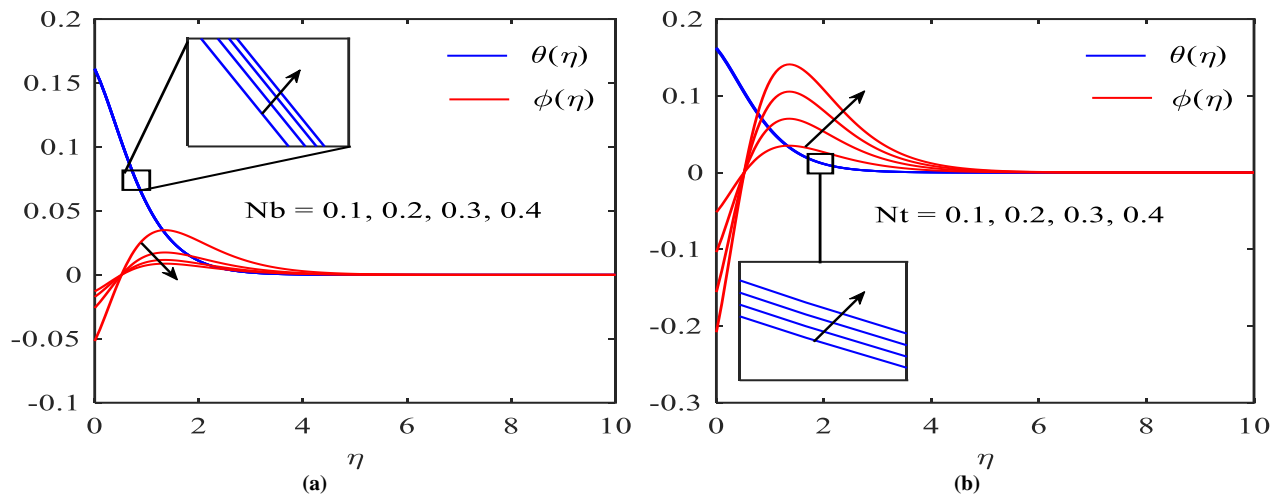


Fig. 7 Effects of Nb and Nt on temperature and nanoparticle volume fraction profiles

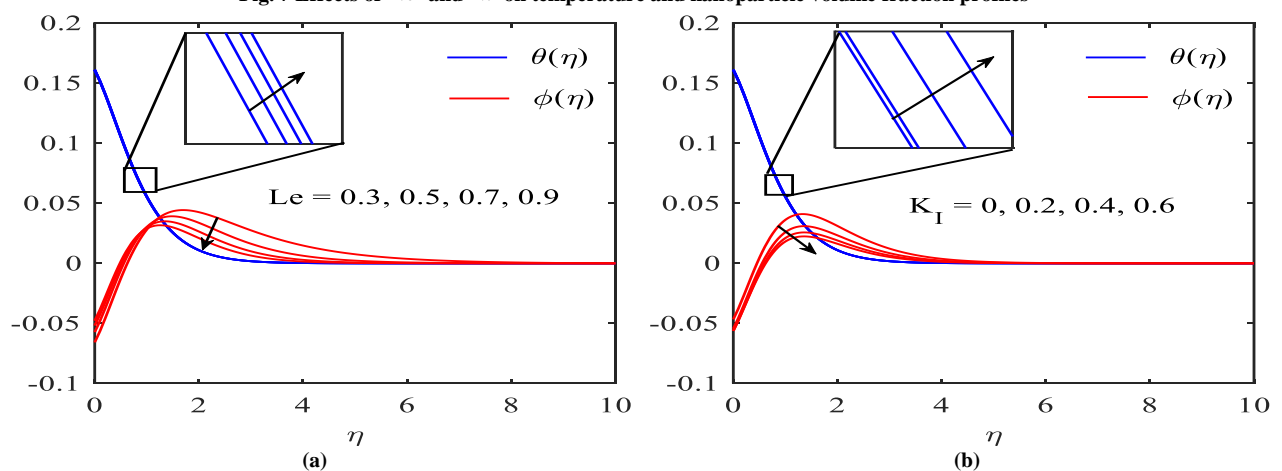


Fig. 8 Effects of Le and K_I on temperature and nanoparticle volume fraction profiles

The behavior of the Brownian motion parameter Nb on the temperature and nanoparticle volume fraction profiles are drawn in Fig. 7a. It is seen that the temperature profile is increasing but reverse behavior is obtained for nanoparticle volume fraction profiles with increasing values of the Brownian motion parameter Nb . This is because that the random motion of the particles enhances by increasing the Brownian motion parameter Nb and, as a result, the temperature profile increases. Figure 7b gives the insight for the influence of the thermophoresis parameter Nt on the temperature and nanoparticle volume fraction profiles. The increase in the thermophoresis parameter Nt leads to the enhancement of both the temperature and nanoparticle volume fraction profiles. The difference between the wall and reference temperatures increases for larger thermophoresis parameter Nt , and the nanoparticles move from hot region to cold region. Hence, the temperature profile increases.

Figure 8a depicts the variation of temperature and nanoparticle volume fraction profiles with coordinate η for various values of Lewis number Le . It is clear from the figure nanoparticle volume fraction profile reduces with an increase in Lewis number, but temperature profile increases. An increase in the values of Lewis number Le corresponds to a weak Brownian diffusion coefficient which results in short penetration depth for nanoparticle volume fraction profile. As a result a rise in Le the nanoparticle volume fraction decreases. It is also noticeable that the nanoparticle volume fraction profile is affected more even for small value of Lewis number Le . Figure 8b shows the influence of the chemical reaction parameter on the temperature and nanoparticle volume fraction profiles within the boundary layer. From this graph, it is observed that the nanoparticle volume fraction reduces but temperature profile increases with an increase in the chemical reaction parameter.

In order to determine the impact of viscous forces at the surface, skin friction is analyzed in Fig. 9a and 9b with respect to the variation of suction/blowing parameter S , power law index n , magnetic parameter M , Weissenberg number We and inclination angle γ . It is observed that skin friction depicts the decreasing behavior for both blowing and suction region. From these figures local skin friction is decreasing with various values of power law index

n , magnetic parameter M and Weissenberg number We and inclination angle γ . In Figs. 10a and 10b, variation is obtained for local Nusselt number with suction/blowing parameter, viscous dissipation parameter, Biot number, Prandtl number and thermophoresis parameter. It is seen that the local Nusselt number is decreasing with increasing values of suction/blowing parameter, viscous dissipation parameter and thermophoresis parameter, but reverse behavior is obtained for Biot number and Prandtl number.

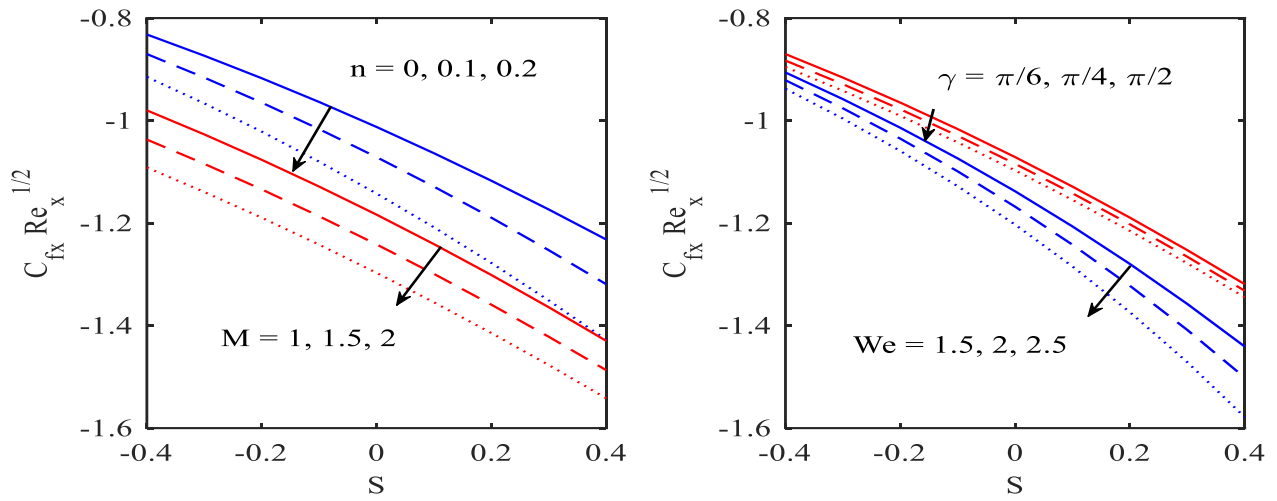


Fig. 9 Variation of skin friction with various values of S, n, M, We and γ

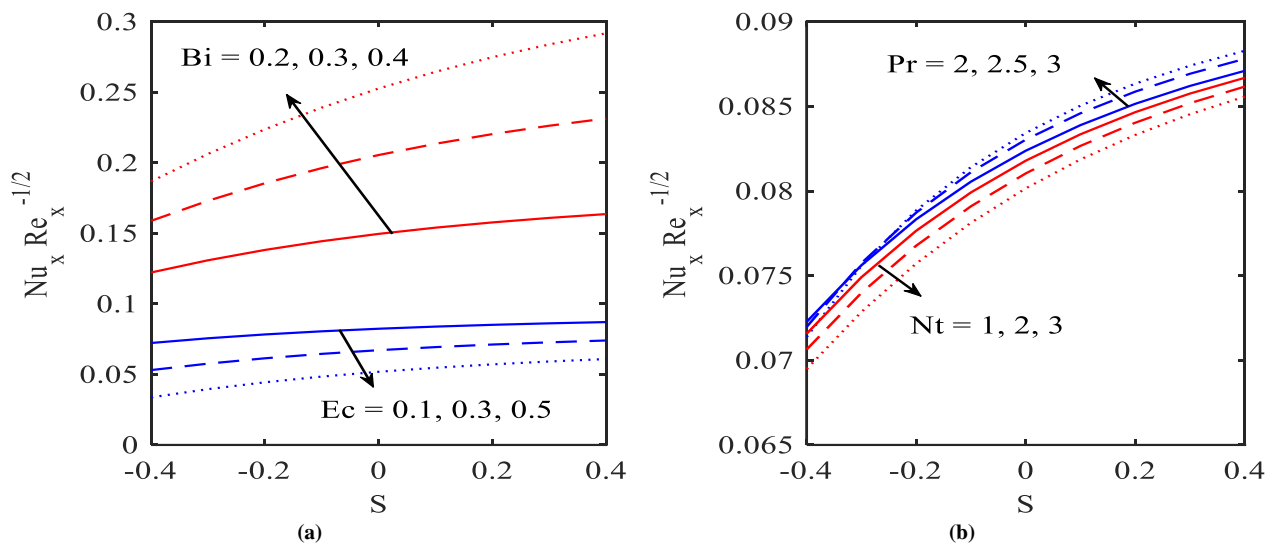


Fig. 10 Variation of skin friction with various values of S, Ec, Bi, Pr and Nt

CONCLUSIONS

In this paper, we studied the impact of inclined magnetic field, viscous dissipation and chemical reaction on MHD boundary layer flow of tangent hyperbolic nanofluid over stretching sheet with suction/blowing and convective boundary condition. The main findings of this study are as follows:

- Velocity profile decreases with increasing magnetic parameter M but temperature and nanoparticle volume fraction profiles are increases in this case.
- Inclined angle γ reduces the velocity profile, but it increases the temperature and nanoparticle volume fraction profiles.
- The surface temperature of a sheet increases with viscous dissipation parameter Ec . This phenomenon is ascribed to a higher effective thermal diffusivity.
- As the thermophoresis parameter Nt enhances, both temperature and nanoparticle volume fraction profiles increases. The effect of Brownian motion Nb is to increase the temperature and decrease the nanoparticle volume fraction profiles.
- The skin friction decreases with the increasing values of S, n, M, We and γ .
- The local Nusselt number decreases with the increasing values of Ec and thermophoresis parameter Nt .

REFERENCES

- [1] BC Sakiadis, Boundary-Layer Behavior on Continuous Solid Surfaces: I. Boundary- Layer Equations for Two-Dimensional and Axisymmetric Flow, *American Institute of Chemical Engineers*, **1961**, 7 (1), 26-28.
- [2] LJ Crane, Flow past a stretching plate, *Zeitschrift für angewandte Mathematik und Physik*, **1970**, 21, 645-647.
- [3] PS Gupta and AS Gupta, Heat and Mass Transfer on a Stretching Sheet with Suction or Blowing, *The Canadian Journal of Chemical Engineering*, **1977**, 55, 744-746.
- [4] E Magyari and B Keller, Heat and Mass Transfer in the Boundary Layers on an Exponentially Stretching Continuous Surface, *Journal of Physics D: Applied Physics*, **1999**, 32, 577-585.
- [5] EMA Elbashbeshy, Heat Transfer over an Exponentially Stretching Continuous Surface with Suction, *Archives of Mechanics*, **2001**, 53, 643-651.
- [6] M Fathizadeh, M Madani, Y Khan, N Faraz, Y Ahmet and S Tutkun, An Effective Modification of the Homotopy Perturbation Method for MHD Viscous Flow over a Stretching Sheet, *Journal of King Saud University - Science*, **2011**, 25 (2), 107-113.
- [7] I Pop and DB Ingham, *Convective Heat Transfer: Mathematical and Computational Modelling of Viscous Fluids and Porous Media*, Pergamon, Amsterdam, **2001**.
- [8] S Nadeem and S Akram, Peristaltic Transport of a Hyperbolic Tangent Fluid Model in an Asymmetric Channel, *Zeitschrift für Naturforschung A*, **2009**, 64a, 559-567.
- [9] AJ Friedman, SJ Dyke and BM Phillips, Over-Driven Control for Large-Scale MR Dampers, *Smart Materials and Structures*, **2013**, 22 (15), 045001-045015.
- [10] S Nadeem and EN Maraj, The Mathematical Analysis for Peristaltic Flow of Hyperbolic Tangent Hyperbolic Fluid in a Curved Channel, *Communication in Theoretical Physics*, **2013**, 59 (6), 729-736.
- [11] NS Akbar, S Nadeem, RU Haq and ZH Khan, Numerical Solutions of Magneto-Hydrodynamic Boundary Layer Flow of Tangent Hyperbolic Fluid Towards a Stretching Sheet, *Indian. Journal of Physics*, **2013**, 87, 1121-1124.
- [12] SUS Choi, Enhancing Thermal Conductivity of Fluids with Nanoparticle, Developments and Applications of Non-Newtonian Flows American Society of Mechanical Engineers, *Central Michigan University*, **1995**, 231, 99-105.
- [13] BC Pak and Y Cho, Hydrodynamic and Heat Transfer Study of Dispersed Fluids with Submicron Metallic Oxide Particles, *Experimental Heat Transfer*, **1998**, 11, 151-170.
- [14] Y Xuan and Q Li, Investigation on Convective Heat Transfer and Flow Features of Nanofluids, *Journal of Heat Transfer*, **2003**, 125 (1), 151-155.
- [15] L Wang and X Wei, Heat Conduction in Nanofluids, *Chaos, Solitons & Fractals*, **2009**, 39 (5), 2211-2215.
- [16] J Buongiorno, Convective Transport in Nanofluids, *Journal of Heat Transfer*, **2010**, 128, 240-250.
- [17] WA Khan and I Pop, Boundary-Layer Flow of a Nanofluid Past a Stretching Sheet, *International Journal of Heat and Mass Transfer*, **2010**, 53, 2477-2483.
- [18] S Akram and S Nadeem, Consequence of Nanofluid on Peristaltic Transport of a Hyperbolic Tangent Fluid Model in the Occurrence of apt (tending) Magnetic Field, *Journal of Magnetism and Magnetic Materials*, **2014**, 358, 183-191.
- [19] N Saidulu and AV Lakshmi, Slip Effects on MHD Flow of Casson Fluid over an Exponentially Stretching Sheet in Presence of Thermal Radiation, Heat Source/Sink and Chemical Reaction, *European Journal of Advances in Engineering and Technology*, **2016**, 3 (1), 47-55.
- [20] P Bala Anki Reddy, Magnetohydrodynamic Flow of a Casson Fluid over an Exponentially Inclined Permeable Stretching Surface with Thermal Radiation and Chemical Reaction, *Ain Shams Engineering Journal*, **2016**, 7, 593-602.
- [21] B Prabhakar, B Shankar and Rizwan UI Haq, Impact of Inclined Lorentz Forces on Tangent Hyperbolic Nanofluid Flow with Zero Normal Flux of Nanoparticles at the Stretching Sheet, *Neural Computing and Applications*, **2016**, DOI 10.1007/s00521-016-2601-4.
- [22] T Hayat, Q Sajid, B Ahmad and M Waqas, Radiative Flow of a Tangent Hyperbolic Fluid with Convective Conditions and Chemical Reaction, *The European Physical Journal Plus*, **2016**, 131, 422.
- [23] T Hayat, M Mumtaz, A Shafiq and A Alsaedi, Stratified Magnetohydrodynamic Flow of Tangent Hyperbolic Nanofluid Induced by Inclined Sheet, *Applied Mathematics and Mechanics -English Edition*, **2017**, 38 (2), 271-288.
- [24] T Salahuddin, Imad Khan, MY Malik, Mair Khan, Arif Hussain and Muhammad Awais, Internal Friction between Fluid Particles of MHD Tangent Hyperbolic Fluid with Heat Generation: Using Coefficients Improved by Cash and Karp, *The European Physical Journal Plus*, **2017**, 132, 205.
- [25] M Waqas, G Bashir, T Hayat and A Alsaedi, On non-Fourier Flux in Nonlinear Stretching Flow of Hyperbolic Tangent Material, *Neural Computing and Applications*, **2017**, DOI 10.1007/s00521-017-3016-6.
- [26] Mair Khan, Arif Hussain, MY Malik, T Salahuddin and Farzana Khan, Boundary Layer Flow of MHD Tangent Hyperbolic Nanofluid over a Stretching Sheet: A Numerical Investigation, *Results in Physics*, **2017**, 7, 2837-2844.
- [27] K Ganesh Kumar, BJ Gireesha, MR Krishnamurthy and NG Rudraswamy, An Unsteady Squeezed Flow of a Tangent Hyperbolic Fluid over a Sensor Surface in the Presence of Variable Thermal Conductivity, *Results in Physics*, **2017**, 7, 3031-3036.
- [28] Wubshet Ibrahim, Magnetohydrodynamics (MHD) Flow of a Tangent Hyperbolic Fluid with Nanoparticles past a Stretching Sheet with Second Order Slip and Convective Boundary Condition, *Results in Physics*, **2017**, 7, 3723-3731.